0013-7227/98/$03.00/0
Endocrinology

Vol. 139, No. 1
Printed in U.S.A.

Spatio-Temporal Expression Patterns of Steroidogenic Acute Regulatory Protein (StAR) During Follicular Development in the Rat Ovary*

TAMAR RONEN-FUHRMANN, RINA TIMBERG, STEVEN R. KING†, KAREN H. HALES‡, DALE B. HALES‡, DOUGLAS M. STOCCO, AND JOSEPH ORLY

Department of Biological Chemistry (T.R.-F., R.T., J.O.), The Alexander Silberman Institute of Life Sciences, The Hebrew University of Jerusalem, Jerusalem 91904, Israel; Department of Cell Biology and Biochemistry (S.R.K., D.M.S.), Texas Tech University Health Sciences Center, Lubbock, Texas 79430; and Department of Physiology (K.H.H., D.B.H.), University of Illinois at Chicago, Chicago, Illinois 60612-7342

ABSTRACT

The steroidogenic acute regulatory protein (StAR) is a vital mitochondrial protein that is indispensable for the synthesis of steroid hormones in the steroidogenic cells of the adrenal cortex and the gonads. Recent studies have shown that StAR enhances the conversion of the substrate for all steroid hormones, cholesterol, into pregnenolone, probably by facilitating cholesterol entry into the inner compartment of the mitochondria where the steroidogenic cytochrome P450scc complex resides. To study the potential of StAR to affect ovarian steroidogenesis during follicular development, we examined the time-dependent expression of StAR protein and messenger RNA in PMSG/human CG (hCG)-treated immature rats. Western blot analyses and immunohistochemical and RT-PCR methodologies have revealed a biphasic expression of StAR in the ovaries responding to hormones. The first peak of StAR expression was generated by PMSG administration and lasted for 24 h. Furthermore, it was restricted to the entire network of the ovarian secondary interstitial tissue, as well as to a fewer scattered theca-interna cells. The second burst of StAR expression was observed in response to the LH surge, as simulated by hCG. This time, StAR was expressed in the entire theca-interna and interstitial tissue, as well as in those granulosa cells that were confined to periovulatory follicles. Immunoelectron microscopy studies revealed the over 90% of StAR antigenic sites are localized in the inner compartments of the mitochondrion, suggesting a rapid removal of StAR precursor from the mitochondrial surface, where it is believed to exert its activity. Altogether, our observations portray dynamic acute alterations of StAR expression during the process of follicular maturation in this animal model. Furthermore, if StAR indeed determines steroidogenic capacities in the ovary, our findings imply that, in immature rats undergoing hormonally induced first ovulation: 1) the early phases of follicular development are supported by androgen production originating from nonfollicular cells; 2) estrogen production in the granulosa cells of Graafian follicles is nourished by a submaximal androgenic output in the theca-interstitial compartments of the ovary. (*Endocrinology* **139:** 303–315, 1998)

TROPHIC hormones stimulate the synthesis of steroid hormones in target tissues through the intermediacy of cAMP (1, 2). cAMP-dependent events lead to expression of the mitochondrial enzymatic complex of cholesterol side chain cleavage cytochrome P450 (P450scc), which executes the first reaction in steroid hormone biosynthesis, *i.e.* the conversion of cholesterol substrate to pregnenolone (1, 3, 4). However, it is now clear that the rate of steroidogenesis in the presence of existing P450scc complex is determined by another protein, designated steroidogenic acute regulatory protein (StAR). StAR has been recently identified as a mitochondrial phosphoprotein (reviewed in Refs. 5–7), which is rapidly induced by trophic hormones and has been implicated as the regulator of cholesterol mobilization into the inner mitochondrial membranes where P450scc resides (8–10). For example, expression of biologically active human recombinant StAR in nonsteroidogenic COS-1 monkey kidney cells was critical for pregnenolone production from cholesterol but did not affect steroidogenesis from a permeable cholesterol substrate like 20α-hydroxyprogesterone (11). StAR is an indispensable protein in hormone regulated steroidogenesis. Moreover, it has been recently been demonstrated that mutations in the gene for the StAR protein are the cause of the potentially lethal disease, congenital lipoid adrenal hyperplasia, in which the afflicted individuals are unable to synthesize steroids to any great extent (12). Such affected infants die shortly after birth, unless treated with steroid hormone replacement therapy (11). In response to trophic hormones and cAMP, StAR is synthesized as a 37-kDa precursor that is rapidly imported into the mitochondria via its N-terminal leader sequence (13). Typical mitochondrial uptake of StAR is associated with processing of StAR to yield a 30-kDa phosphoprotein, the function of which, if any, is still obscure (8–10, 14, 15).

To test the effect of hormones on StAR levels in the ovary, the present study was designed to follow the expression pattern of StAR through the follicular phase of the ovarian response to gonadotropins in the rat and compare it with the levels of P450scc, the enzyme responsible for the conversion

Received June 4, 1997.
Address all correspondence and requests for reprints to: Dr. Joseph Orly, Department of Biological Chemistry, The Alexander Silberman Institute of Life Sciences, The Hebrew University of Jerusalem, Jerusalem 91904, Israel. E-mail: orly@vms.huji.ac.il.
* This work was supported by the United States-Israel Binational Sciences Foundation Grant 95–00350 (to J.O.); NIH Grant HD-17481 (to D.M.S.).
† Supported by NIH Grant HD-07271.
‡ Supported by NIH Grant HD 27571.

of cholesterol to pregnenolone. Furthermore, assuming that StAR is critical for the steroidogenic activity of the ovary, we were interested in examining the potential correlations between the levels of StAR, P450scc, and other steroidogenic cytochromes with the known plasma levels of ovarian steroids that are found throughout follicular development in the rat. To this end, PMSG/human CG (hCG)-treated prepubertal females served as an interesting experimental model because, at 24–26 days of age, the functional cells of the rat ovary are considered naive due to low endogenous plasma gonadotropin levels (16). Yet, such ovaries are developmentally primed for a robust response to gonadotropin administration, resulting in ovulation of multiple follicles. Therefore, we anticipated that the superovulating rat model should enable the study of cell-specific StAR expression in the different cellular compartments of the rat ovary during the process of follicular maturation toward ovulation.

Our previous studies of P450scc expression (17) have shown that the superovulating rat model proved to be instrumental in shedding light on the mechanism of ovarian steroidogenesis, which, unlike other steroid-producing organs, depends on the concerted action of different cell types responding to more than one trophic hormone (18, 19). Those cell types are: 1) the intrafollicular granulosa and cumulus cells endowed with FSH responsiveness at early stages of follicular development (17, 20, 21); for example, priming with FSH confers granulosa cell induction of various genes expressed before the LH surge (22), including cytochrome P450 aromatase (P450arom) catalyzing estrogen synthesis, and high levels of LH receptors (23, 24); 2) the follicular theca-interna cells, which constitutively possess LH receptors, P450scc and androgen producing cytochrome P450 17, 20 lyase (P45017α; 24–26); and 3) the secondary interstitial cells, which originate from hypertrophied theca interna cells of atretic follicles (27, 28) and are, therefore, functionally related to theca cells. Both the interstitial cells and the theca-interna cells produce androgens but lack the ability to further process those to estrogens. By contrast, the granulosa cells lack P45017α but can use the theca-derived androgens as substrate for aromatization to estrogens by their FSH-inducible P450arom (17, 22).

The present study describes a spatio-temporal expression pattern of StAR observed in the different ovarian cell types which is novel. The observed integrated expression pattern of StAR, P450scc, P45017α, and P450arom suggest a revised model for the cellular organization of ovarian steroidogenesis during the process of follicular maturation.

Materials and Methods

Materials

Pregnant mare serum gonadotropin (PMSG 600) was purchased from Intervet (Angers, France) and human CG from Organon Special Chemicals (West Orange, NJ). Ovine FSH (NIDDK-oFSH-20; FSH RIA potency = 1.31 ng/ng in NIH-FSH-RP-1 terms, or *in vivo* biological potency of 4453 IU/mg in terms of W.H.O. 2nd IRP-HMG; LH contamination, 0.07 ng/ng in oLH NIDDK-23 terms) and ovine LH (NIADDK-oLH 26; biological potency - 2.3 NIH-LH-S1 U/mg; FSH contamination less than 0.5% by weight) were kindly provided by The Institute of Arthritis, Metabolism and Digestive Diseases (Bethesda, MD). Insulin (I-5500), transferrin (T-4515), hydrocortisone (H-4001) and phenylmethylsulfonylfluoride were obtained from Sigma Chemical Co. (St. Louis, MO). DMEM and Ham's F-12 were from Gibco BRL, Life Technologies (Paisley, Scotland). Collagenase/Dispase (Vibrio alginolyticus/Bacillus polymyxa) was from Boehringer Mannheim Biochemica (Mannheim, Germany).

Immunoreagents

StAR. All Western blot analyses were conducted by use of a polyclonal rabbit antiserum raised against a peptide fragment (amino acids 88–98) of the 30-kDa mouse StAR protein (13). For immunofluorescence histochemical studies and immuno-electron microscopy, we applied a polyclonal rabbit antiserum to the recombinant mature mouse StAR protein. To this end, the mouse StAR complementary DNA (cDNA) was digested with *Sma*I and ligated to *Bam*HI linkers. The DNA was digested with *Bam*HI, and the 1273-bp fragment was cloned into the dephosphorylated *Bam*HI site of GEX2T (Pharmacia, Piscatway, NJ). The linker sequences (5′-CGCGGATCCGCG-3′) were added to maintain the reading frame and add an alanine residue between the thrombin cleavage site of the vector and amino acid 46 of StAR. This removes all but two amino acid residues of the predicted signal peptide resulting in a fusion of the mature 30-kDa form of StAR with glutathione S-transferase. The protein was expressed in bacteria and purified by glutathione affinity chromatography and injected into rabbits. A specific, high titer antibody was elicited that was suitable for immunohistochemistry.

P450scc. A polyclonal rabbit antiserum to rat P450scc was prepared and previously characterized (29). Other antisera included commercially available lissamine rhodamine-conjugated AffiniPure goat antirabbit IgG (H + L), peroxidase-conjugated AffiniPure goat antimouse IgG (H + L) and 12 nm gold-labeled goat antirabbit IgG (Jackson ImmunoResearch Inc., West Grove, PA).

Animals

Intact, immature female Sprage-Dawley rats (21 days old) were obtained from Harlan (Jerusalem, Israel) and maintained under 16-h light, 8-h dark schedule with food and water *ad libitum*. Animals were treated in accordance with the NIH Guide for the Care and Use of Laboratory Animals. All protocols had the approval of the Institutional Committee on Animal Care and Use, The Alexander Silverman Institute of Life Sciences, The Hebrew University of Jerusalem.

In vivo treatments before tissue/cell extracts

Twenty-four-day-old rats were injected at 1000 h with sc administered 15 IU PMSG; 50 h later, simulation of the LH surge was achieved by hCG (4 IU) administration (sc). Under such conditions, 20–30 oocytes ovulate 12–14 h after hCG administration (21). At the indicated time points the animals were killed by cervical dislocation, the ovaries were removed, trimmed free of fat and stored in liquid nitrogen until further processing for extraction of proteins or total RNA. Four rats were used for each of the time points between 0–36 h postPMSG administration, whereas two animals were killed to obtain the ovaries during advanced stages of follicular development. From each animal, one of the ovaries was processed for protein extraction and Western blot analysis, whereas the collateral organ was extracted with RNAzol B^{TM} (Cinna Biotex, Houston, TX), for total RNA preparation.

RT-PCR analysis

Total RNA was prepared by RNAzol B extraction after homogenization of the tissue (100–300 μl/ovary) by 5–7 gentle strokes of Dounce homogenizer (Wheaton, Millville, NJ). Further procedures were conducted according to the manufacturer's instructions. RNA samples were precipitated in 70% ethanol and stored at −20 C until use. Dried RNA pellets were dissolved in water containing 0.1% diethylpyrocarbonate (DEPC), and quantified by measuring the absorbency at 260 nm. Aliquots containing 50–100 ng RNA were assayed by relative-quantitative RT-PCR procedure as previously described (30, 31). Briefly, RT was performed for 75 min at 42 C using 500 ng pd$(T)_{12-18}$ primers (Pharmacia no. 27–7858, Piscatway, NJ) and 0.25 unit of AMV reverse transcriptase (Promega no. M510, Madison, WI); for RT-PCR determination of the rat StAR transcript, it was found to be essential that rat StAR reverse

oligonucleotide B be added during RT. PCR was conducted in the presence of 2 μCi of [α-^{32}P]-deoxy-ATP (3000 Ci/mmol), all four dNTPs (200 μM) and 500 ng of the appropriate oligonucleotide primers (50–60 pmol); oligonucleotide primers for the ribosomal protein L19 served as an internal control. Following the PCR reaction (20 cycles, annealing temperature of 65 C), tracking dye gel buffer was added to 20–40 μl of the PCR reaction mixture (100 μl) for further analysis by electrophoresis on 5% polyacrylamide gels (30). The dried gels were quantified using a Fuji Bio-Imaging analyzer (BAS-1000, Fuji Photo Film Co., Tokyo 106, Japan). The radioactivity in each of the PCR bands was normalized to the radioactivity of the ribosomal protein L19 band that was used as an internal control. Gels were also exposed to *RX* medical x-ray film (Fuji Photo Film, Tokyo 106, Japan) for 2–16 h at −80 C and developed by a X-Omat processor.

PCR oligonucleotide primer pairs were designed based on known cDNA sequences of the various target genes, so that the expected PCR products would be 246 bp for the rat StAR cDNA (Ref. 32 and our unpublished sequence); 536 bp for the rat P450scc; 271 bp for the rat P450arom; 361 bp for rat P45017α, and 194 bp for the rat RPL19. Forward (A, sense) and reverse (B, antisense) primers were: rat StAR A, 5′-GCAGCAGGCAACCTGGTG and StAR B, 5′-TGATTGTCTTCG-GCAGCC; rat P45017α A, 5′-GGGGCAGGCATAGAGACAACT and P45017α B, GCCTGAGCGCTTCTTAGATCC; other primer sequence for RT-PCR determination of P450scc, P450arom and L19 messenger RNA (mRNA) were previously published (30).

Western blot analysis

Whole ovary proteins were extracted in RIPA buffer (150 mM NaCl, 50 mM Tris-HCl, pH 7.5, 1% Triton X-100, 0.5% deoxycholate, 0.1% SDS and 0.1 mM of freshly added phenylmethylsulfonylfluoride) by homogenization (100 μl/ovary) in a Dounce homogenizer, as described for extraction of RNA above. For determination of cell-specific expression of StAR, first, granulosa cells were expressed by needle pricking as previously described (31), and the resulting residual tissue was designated as a mixture of theca-interna and secondary interstitial (theca-interstitial) cells. Both cell types were further extracted by homogenization in RIPA buffer. After homogenization, samples were incubated for 30 min on ice, vortexed, and centrifuged for 5 min at 14,000 $\times$ *g*. The supernatant was separated and protein concentration was determined by a modification of the protein assay according to Bradford (33). SDS-PAGE sample buffer (31 mM Tris-HCl pH 6.8, 1% SDS, 0.05 mM EDTA, 5% glycerol, and 0.003% bromophenol blue) was added to the samples, and after heating for 5 min at 95 C, samples were stored at −20 C until use.

Samples were electrophoresed on a 10% mini gel by standard SDS-PAGE procedures (34), along with prestained mol wt markers (Novex MultiMark, Novex, San Diego, CA). Gels were electrophoresed at 30 mA/mm at 4 C using a running buffer that included 12.5 mM Tris base, 96 mM glycine, and 0.01% SDS. The proteins were electrophoretically transferred to Optitran BA-S 85 nitro-cellulose membrane (Schleicher & Schuell, Dassel, Germany) using a semidry electro-transfer apparatus (E&K Scientific Products, Saratoga, CA). Protein transfer was conducted for 45 min at 3 mA/cm^2 in a modified buffer consisting of 48 mM Tris-base, 39 mM glycine, 0.04% SDS, and 20% methanol (35). The membrane was blocked by a 30-min incubation in blocking buffer (PBS buffer containing 0.1% Tween 20 and 5% nonfat dry milk), followed by an overnight incubation with anti-StAR (1:5000) and anti P450scc (1:10,000). After three washes for 5 min each with PBS/Tween buffer (as above, without milk), the membranes were incubated for 1 h with peroxidase-conjugated goat antirabbit IgG (1:10,000 dilution). Specific signals were detected by chemiluminescence using the LumiGlo substrate (New England BioLabs, Beverly, MA).

Analysis of chemiluminescence Western blot data

Quantitation of chemiluminescence signals on x-ray films was performed as follows: chemiluminescence pseudo-autoradiograms were scanned using a Power Macintosh computer (6200/75, Apple Computer Corp., Cupertino, CA) scanner (AV 6120, Avision Inc. Hsinchu, Taiwan) using a green filter, 150 dpi resolution, 256 gray-levels, 10% brightness, 30% contrast and $\gamma = 2$. Quantification of scanned images was performed according to the user manual of the public domain NIH Image Program (developed at the U.S. National Institutes of Health and available on the Internet at http://rsb.info.nih.gov/nih-image/).

COS cell expression of recombinant StAR

COS cells (2×10^6 cells/0.8 ml) were transfected by electroporation using 30 μg pCMV(StAR) DNA (14) as previously described (31). The electroporated cells were seeded onto 13 mm round glass slides and placed in the wells of a 24-well plate (Nunc, Denmark). After a 48-h incubation in DMEM:F-12 medium containing 5% FCS (Biological Industries, Kibbutz Beit-Haemek, Israel), the cell monolayers were fixed and immunofluorescently stained as described below.

Primary cell cultures

Granulosa cells were isolated by needle pricking and the resulting residual tissue, comprised of theca-interstitial cells was further dissociated into a single cell suspension by collagenase-DNase treatment as previously described (19). Both granulosa cells and theca-interstitial cell cultures were plated onto serum-coated round glass slides prepared for serum free culture as previously described (31). Serum-free medium (4F medium) consisted of 1:1 (vol/vol) mixture of DMEM:F-12 nutrient media (36), supplemented with insulin, transferrin and hydrocortisone (31). Both cell types were grown in 24-well plates (Nunc Copenhagen, Denmark) incubated at 37 C in a humidified incubator 95% air/5% CO_2. Theca-interstitial cells were treated for 5 h with 50 ng/ml LH, whereas 100 ng/ml FSH was added to the granulosa cell cultures, followed by further processing for immunofluorescence staining.

Immunofluorescence staining

The immunofluorescence staining procedure used to visualize mitochondrial StAR in primary cultures and transiently transfected COS cells has been described previously (37). Also, immunofluorescence staining of ovarian cryosections was performed as previously described (38). Polyclonal rabbit antiserum to recombinant murine StAR (1:50) and lissamine-rhodamine labeled goat (IgG) antirabbit IgG (1:20) were used for both of the histochemical and cytochemical studies.

Electron microscopy and analysis of the data

Rat ovaries were trimmed free of fat and small fragments were fixed in freshly prepared PBS containing 1% glutaraldehyde and 3% p-formaldehyde. After an overnight incubation at 4 C (29, 39), preparation of the tissue blocks in LR White resin (London Resin Co., Bassingstoke, UK) was performed as recently described (29). Thin sections were incubated with 1:20 dilution of antirecombinant mouse StAR, followed by incubation with 1:10 dilution of gold labeled goat antirabbit IgG, as previously described (39).

The relative partitioning of gold particles observed in the different submitochondrial compartments (legend of Fig. 6) was assessed by counting high power micrographs of mitochondria, as indicated in the figure legends. Results are expressed as the mean ± SE. For measurements comparing StAR distribution in the adrenal and ovary, significance of StAR localization was determined through the use of the Duncan's multiple range test. A value of $P < 0.05$ was considered as statistically significant.

Results

Temporal changes in StAR expression

The objective of this study was to characterize the pattern of StAR expression throughout the process of follicular development in the rat ovary. First, we compared the relative transcript levels of StAR, P450scc, P45017α, and P450arom in whole ovary extracts prepared time dependently following the administration of PMSG to prepubertal rats. For the analysis of mRNA, we applied a semiquantitative RT-PCR assay we have previously characterized to study the effects of protein kinase inhibitors on expression of the ovarian steroidogenic P450s (30). Figure 1 shows that a relative quan-

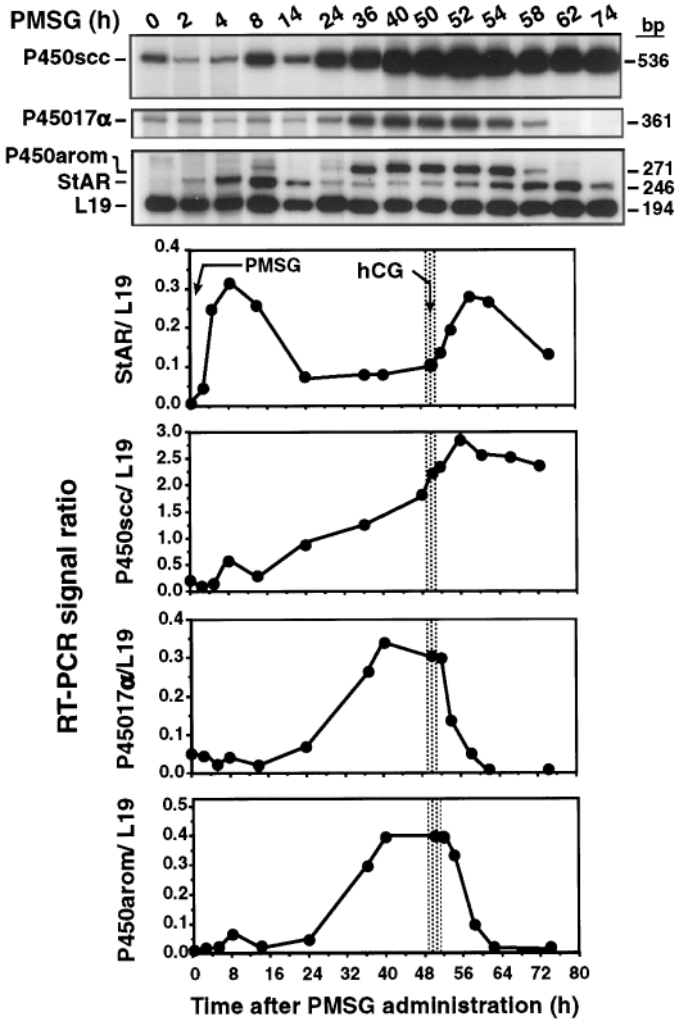

FIG. 1. PMSG/hCG induced accumulation of StAR, P450scc, P45017α, and P450arom mRNA. PMSG (15 IU) was administered at 1000 h to 25-day-old rats, and 50 h later the LH surge was simulated by hCG administration (4 IU). At the indicated time points, extracts of whole ovarian tissue were prepared (*Materials and Methods*), and the transcript levels of StAR and the steroidogenic cytochromes were determined by RT-PCR using 50 ng of total RNA (*Materials and Methods*). Control animals were not treated with the gonadotropin (time 0). *Top panels*, autoradiograms depicting the amplified PCR signals obtained for each set of primers. The level of the ribosomal protein L19 (L19) PCR products, which is not affected by hormonal treatments, served for quantitative normalization of the target gene products, as described in the *Materials and Methods*. The phosphorimager data are shown in the *bottom panels*. The data are representative of two independent experiments repeated with similar results.

titation is indeed feasible for each of the individual transcripts because the housekeeping reference gene of choice, the ribosomal protein L19 (40, 41), was not affected by the *in vivo* hormonal treatments (panel A). By contrast, StAR mRNA levels increased in a biphasic pattern. Before PMSG administration, StAR mRNA levels were barely detectable under the given conditions of our RT-PCR assay, for which we have confirmed linearity of all PCR products produced at 20–120 ng RNA input (not shown). PMSG caused a rapid rise in StAR transcript level, observed much earlier than any other of the steroidogenic P450s (Fig. 1). Interestingly, a few hours later, the level of StAR mRNA markedly dropped to 20% of its maximal value, and remained as such until after administration of hCG. Exogenous hCG simulation of the LH surge elicited the second peak in StAR mRNA levels, which reached maximal values within 8 h of hormone administration.

The expression pattern of P450scc mRNA differed substantially from that of StAR. A marked basal level of P450scc mRNA was observed even before PMSG treatment and levels gradually increased and attained maximal values 8 h after hCG administration. A similar pre-PMSG level of transcript was also observed for P45017α mRNA. However, following the gonadotropin administration, P45017α and P450arom transcript levels provided a third type of time-dependent response to PMSG, comprising a single peak, synchronously elevated 10 h before hCG administration. Thereafter, as a result of hCG administration, both P45017α and P450arom mRNAs precipitously declined and were totally lost at the time of ovulation (Fig. 1), which occurred 64 h after initiation of follicular development by PMSG.

Figure 2 shows that StAR protein pattern followed the profile of StAR mRNA, with a biphasic rise in the levels of StAR protein typically seen in the ovarian homogenates. The peak levels of StAR protein observed 8–16 h after PMSG

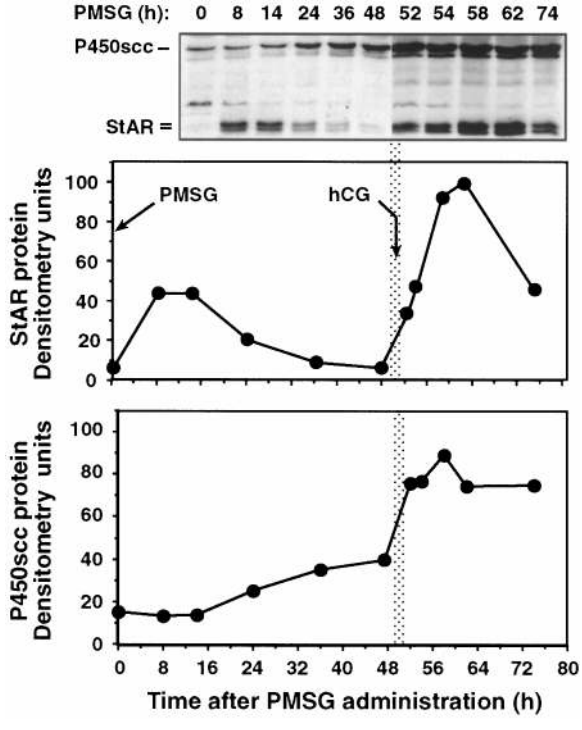

FIG. 2. PMSG-induced accumulation of StAR and P450scc protein. PMSG and hCG were administered as described in Fig. 1, and protein extracts were time dependently prepared from whole ovaries obtained as described in *Materials and Methods*. *Top*, Western blot analysis of cell extracts (20 μg) subjected to SDS-PAGE and developed by ECL reaction. P450scc (54 kDa) and StAR doublet bands (30 kDa) were depicted by a concomitant incubation with the P450scc and StAR antisera. *Bottom*, densitometric analysis of the ECL signals was performed as described in *Materials and Methods*. This experiment was repeated twice with similar results.

administration declined, thereafter, to nearly basal level at 36 h. Again, P450scc levels were markedly different than those of StAR, depicting three phases of P450scc accumulation in the ovary: no apparent change in P450scc levels during the first hour after PMSG administration, followed by a 2.5-fold gradual increase in accumulating P450scc until hCG administration, and a final immediate rise in the cytochrome levels responding to hCG. This pattern fully confirmed our earlier characterization of P450scc protein levels observed during follicular development (38).

Cell specific expression of StAR

To elucidate which of the ovarian cell types expressed StAR throughout its biphasic pattern, we attempted to isolate pure granulosa cells free of the residual tissue, which comprises the theca interna and secondary interstitial compartments of the ovary. To this end, PMSG/hCG treated animals were killed at selected time points and cell-specific proteins were examined by Western blot analysis. Figure 3 clearly shows that the first wave of StAR expression was solely confined to the theca-interstitial cells (lanes 8–9); granulosa cells did not express StAR at this stage of follicular development (lanes 2–3). However, after hCG administration, both the granulosa and the theca-interstitial cell types joined in synchronized production of StAR observed 8 h after simulation of the LH surge by hCG (lanes 5 and 11). Moreover, in full confirmation of the results described in Fig. 2, a typical attenuation of StAR protein always followed hormone induced stimulation, be it the theca-interstitial cells responding to PMSG (lane 10), or the post hCG response of all cell types

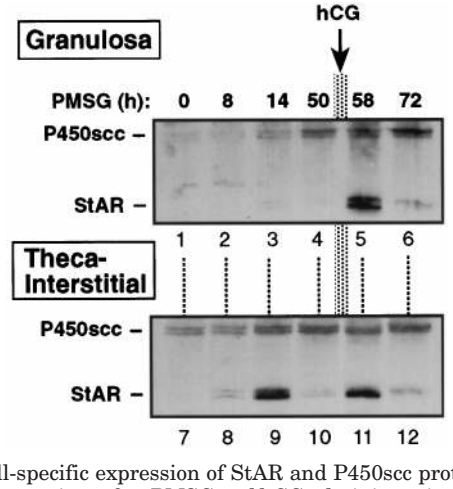

FIG. 3. Cell-specific expression of StAR and P450scc protein. At the indicated time points after PMSG and hCG administration, granulosa cells were isolated by needle pricking so that the residual tissue held by the extracellular matrix consisted of theca and secondary interstitial cells. Pooled cell extracts from triplicate (0–14 h) or duplicate animals (50–72 h) were prepared for each time point. Protein extracts were prepared as described in *Materials and Methods*. Twenty-microgram samples were subjected to Western blot analysis using a concomitant incubation with StAR and P450scc antisera. The electrotransferred protein blot was developed by ECL reaction. *Top panel*, ECL signals obtained for the expression of StAR and P450scc in the granulosa cells; *bottom panel*, time-dependent levels of StAR and P450scc in the isolated theca-interstitial cells (residual tissue). Similar results were obtained in three independent experiments of this kind.

losing StAR in the periovulatory follicles and early phases of corpus luteum formation (lanes 6, 12). Interestingly, in all cases, StAR patterns were independent of the P450scc profiles. For example, before hCG administration, granulosa cells were devoid of StAR although P450scc was already observable (lane 4), and so was the pattern in theca-interstitial cells, which partially lost StAR expression at this preovulatory phase of follicular development, despite their apparent high content of P450scc (lane 10).

Spatio-temporal localization of StAR

In light of the dynamic changes in StAR levels during follicular development, immunohistochemical localization was essential to directly reveal cell-specific patterns of StAR expression in the context of the intact tissue. Additionally, only direct immunolocalization evidence as such, could exclude potential imperfections associated with the biochemical procedure we used to isolate individual ovarian cell types, as shown in Fig. 3. For immunohistochemical studies, we used an antiserum raised against bacterially expressed recombinant murine StAR (*Materials and Methods*), which was more adequate for cryosection labeling than the anti-peptide antiserum used for Western analysis. First, using this new antiserum for immunocytochemical staining of transiently transfected COS-1 cells, we positively confirmed a specific mitochondrial decoration by StAR (Fig. 4A); no nuclear, or possible nonspecific cytoplasmic signals could be detected in the transfected COS cells. The specificity of this antiserum was also validated when StAR staining patterns were examined in LH-responsive cultured theca-interstitial cells (Fig. 4B), or primary granulosa cells treated with FSH (Fig. 4C). Then we applied this antiserum to immunohistochemical localization of StAR in ovarian cryosections.

Figure 5A illustrates a median cryosection of ovary from a 25-day-old rat before PMSG administration. At this time, StAR was not detected by immunohistochemical staining. However, 9 h after gonadotropin treatment, a bright pattern of StAR staining was confined to the interstitial cells, some of the theca cells and atretic follicles (Fig. 5B). Thereafter, the immunohistochemical evidence shown in panel C fully corroborated the biochemical findings indicating that at a later time, before hCG administration, StAR levels in the theca-interstitial compartment were reduced markedly. Shortly after hCG administration, high StAR expression levels resumed in the all-ovarian interstitium, as shown in Fig. 5D. Moreover, StAR was also observed in the theca interna layers in the entire population of the antral follicles (Fig. 5D). Interestingly, at this phase of follicular development, usually perceived as the onset of the luteinization process, high levels of StAR antigen were also expressed in the the granulosa cells. However, a closer examination revealed that in the latter cell type, StAR expression was strictly confined to periovulatory follicles, whereas nonovulating follicles were devoid of StAR in their granulosa cell layers (Fig. 5D).

Submitochondrial localization of StAR

We have previously shown that in cells of the rat adrenal fasciculata zone, 96% of StAR antigenic sites in the mitochondrion localized to the inner compartments of the or-

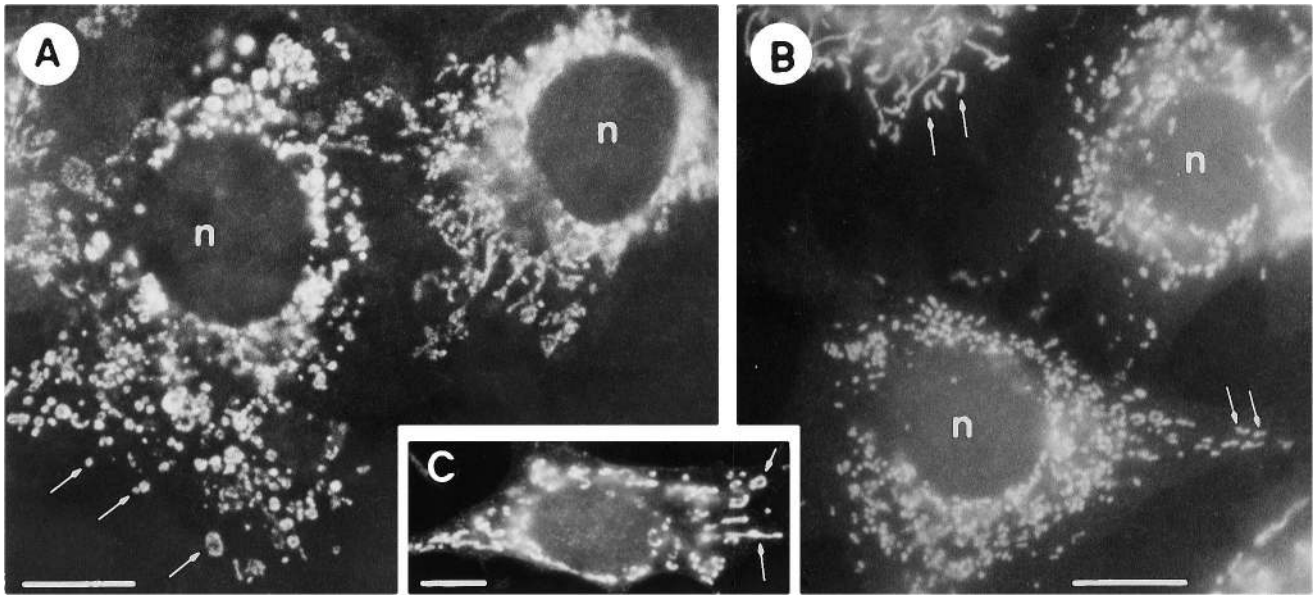

FIG. 4. Immunofluorescence visualization of mitochondrial StAR. A, COS-1 cells were transfected by electroporation with a pCMV(StAR) construct as described in *Materials and Methods*. After 40 h in culture, the cell monolayers were fixed and immunofluorescently stained using recombinant StAR antiserum (*Materials and Methods*). Note the mitochondria (*arrows*) of *dotted* or *circular shapes*. No staining was observed in the nuclei (n), or the cell cytoplasm. B, Similar staining patterns of StAR in isolated primary theca-interstitial cells in culture (*Materials and Methods*). Cells were fixed and stained 5 h after the addition of oLH. *Arrows* depict StAR-decorated mitochondria. C, A comparison with FSH treated (24 h) primary granulosa cell isolated by needle pricking and stained with the antipeptide serum used for Western blot analysis (14). Clearly, the depicted staining characteristics were similar to those shown in panels A and B. *Bars* represent 30, 20, and 10 μm in A–C, respectively.

ganelle (14), and StAR was not confined to the mitochondrial outer membrane, where it is thought to have its biological effect related to cholesterol delivery. Considering the fact that the mechanism of StAR action is still far from being understood, visualization of submitochondrial distribution of StAR could provide further constructive information regarding this issue. Therefore, the ultrastructural localization of ovarian StAR was studied by immuno-gold electron microscopy, in an attempt to document both the granulosa and the interstitial cell types at two critical time points during follicular development (Fig. 6). Nine hours after PMSG administration, granulosa cells from a typical tertiary follicle (panel A) were devoid of StAR expression and the lamellar cristae of their mitochondria marked their non-differentiated status. By contrast, the mitochondria of PMSG-responsive interstitial cells were heavily decorated with StAR-associated colloidal gold particles (panel B), thus fully confirming our immunofluorescence studies. Moreover, large lipid droplets and the tubular-vesicular architecture of the mitochondrial cristae provided structural evidence that these androgen producing cells (28) were fully capable of steroid hormone synthesis as early as 9 h following PMSG administration. Further, ultrastructural examination of ovarian sections prepared 8 h after hCG administration depicted steroidogenic differentiation of mitochondria in both the granulosa and theca-interstitial cell types; panel C shows typical StAR-expressing luteinizing granulosa cells, and panel D depicts a differentiated theca cell of a periovulatory follicle.

Analysis of high power micrographs depicting several cells, which retained good ultrastructural preservation of their mitochondria, enabled a quantitative determination of StAR localization in the different submitochondrial compartments. Based on the high resolution demonstrated in the *insets* of panel D, five categories of StAR localization were determined (legend of Fig. 6D), and the relative distribution of StAR was assessed (Fig. 7). Such analysis revealed that in the ovarian cells, no more than 8% of StAR antigenic sites were associated with the outer membranes of the mitochondrion. Inside the organelle, a total of 77% of the gold particles labeled the matrix, or were apparently anchored to the matrix side of the cristae membranes. Finally, some of StAR-associated particles (14%) were also found in the intermembrane spaces, or were seemingly anchored to the inner face of the cristae membranes.

We also examined the distribution of StAR antigenic sites in mitochondria of adreno-cortical fasciculata cells (Fig. 7), using the same antiserum to recombinant murine StAR. When the ovarian and the adrenal tissue sections were compared for the distribution of the gold particles in the different submitochondrial categories, statistically significant differences were observed for StAR localization: the percentage of particles localized in the matrix of ovarian cells was markedly higher (2.1-fold) than that observed for the matrix associated StAR in the adrenal ($P < 0.05$). Conversely, nearly 45% of the adrenal antigenic sites of StAR localized in the intermembrane spaces, or facing these spaces in the vesicular cristae, whereas less than 15% of the particles were found to reside in this compartment in the ovarian cells (Fig. 7).

Synthesis of StAR protein: the acute response

The attenuation of StAR mRNA and protein levels that followed the initial response of the interstitial cells to PMSG was rather unexpected and occurred for no immediately

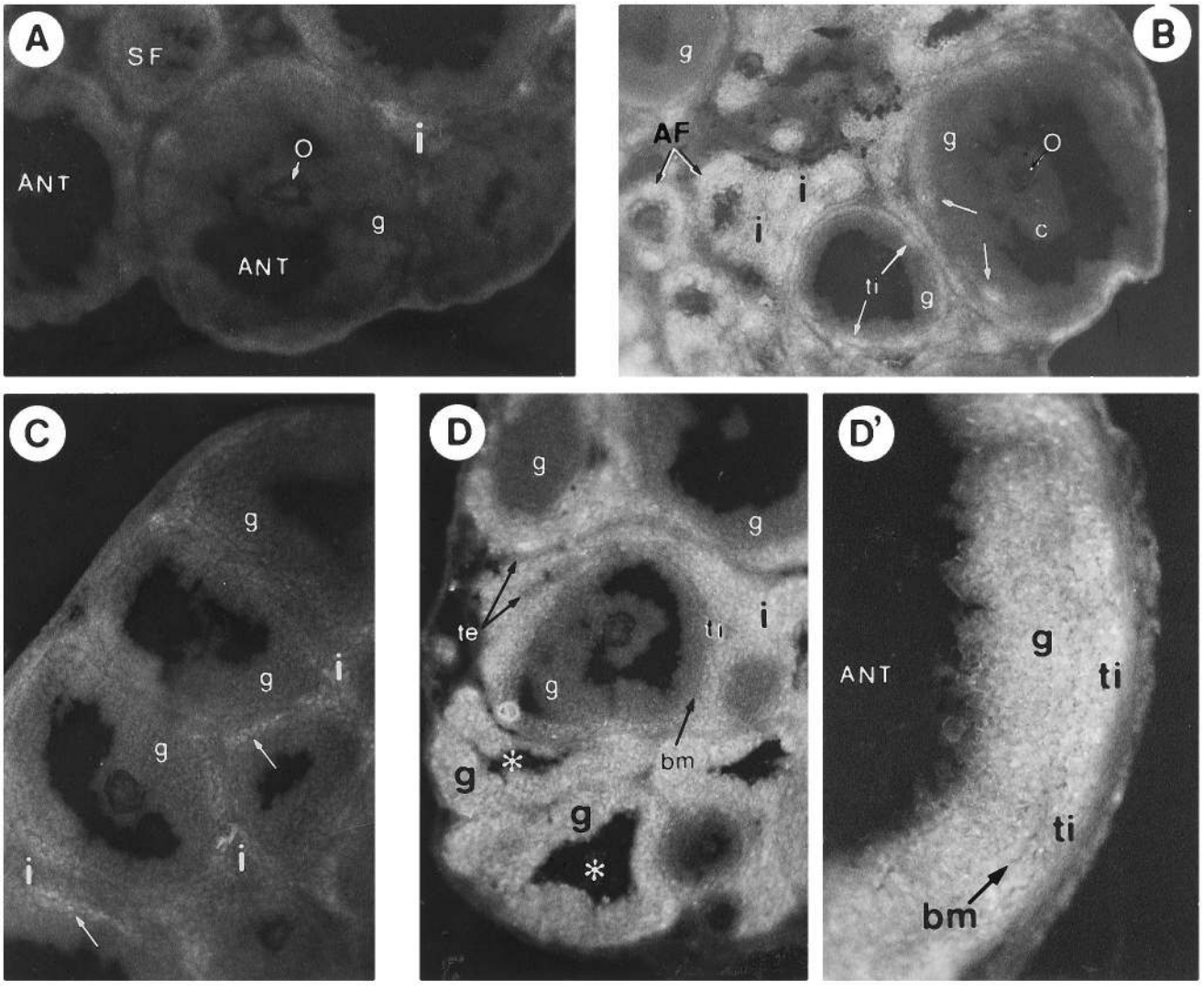

FIG. 5. Immunohistochemical distribution of StAR during follicular development. PMSG was administered to 25-day-old rats, followed by hCG treatment given 50 h later. At selected time intervals, ovaries were cryosectioned and immunofluorescently stained with antiserum to bacterially expressed StAR as in Fig. 4. A, StAR was not detectable before PMSG administration. ANT, antrum in a small antral follicle; g, and O, granulosa layers and oocyte, respectively; SF, small preantral follicle; i, interstitial tissue. B, Ovarian section taken 9 h after PMSG administration. Note ample expression of StAR in interstitium (i), atretic follicles (AF), and some cells of the theca interna layers (ti, *white arrows*). Note lack of StAR expression in the granulosa cells (g) of all follicles. c, cumulus cells. C, Thirty-six hours after PMSG administration, StAR levels markedly reduced in the interstitium (i) and theca-interna cells (*white arrows*). g, granulosa cells. D, Eight hours after hCG administration, StAR heavily labeled the interstitial cells (i), and theca interna (ti) cells of all follicles. By contrast, StAR labeling in the granulosa cells (*black printed g*) was confined to two periovulatory follicles (*), which were sectioned grazing to their surface. Note the apparent lack of StAR expression in granulosa cells of nonovulatory follicles (*white printed g*). bm, Basement membrane; te, fibroblast-like theca-externa cells devoid of StAR, or other steroidogenic enzymes (38). D, Higher magnification of a periovulatory follicular wall depicting high levels of StAR labeling in the granulosa cells (g) and theca interna layers (ti). ANT, antrum; bm, basement membrane. Magnifications, A and B, ×84; C and D, ×50; ×120.

apparent reason. Yet, we could not exclude the possibility that a short half life of the gonadotropins, or alternatively, desensitization of the LH receptors may have caused the observed loss of StAR expression in these cells. To test these possibilities under *in vivo* conditions, we administered a premature hCG bolus (4 IU), commencing 24 h after PMSG administration and followed the mRNA and protein patterns of StAR and P450scc in the boosted animals; control animals were treated as usual by a single PMSG dose. The hCG boost demonstrated the capacity of this hormone to restore StAR protein levels that had been declining (Fig. 8A). Nevertheless, this restoration did not last more than 10 h, after which a subsequent loss of StAR protein did occur. Interestingly, the hCG boost did not restore high levels of StAR mRNA, as shown in Fig. 8B. In this respect, it is also noteworthy that the hCG boost did not significantly affect the P450scc protein (Fig. 8A) or mRNA (not shown).

Discussion

Unlike the continuous nature of steroid hormone secretion from the corpus luteum, placenta and testes, the steroid hormones produced by the ovary have been demonstrated to cycle with remarkable changes in amplitude and appear to

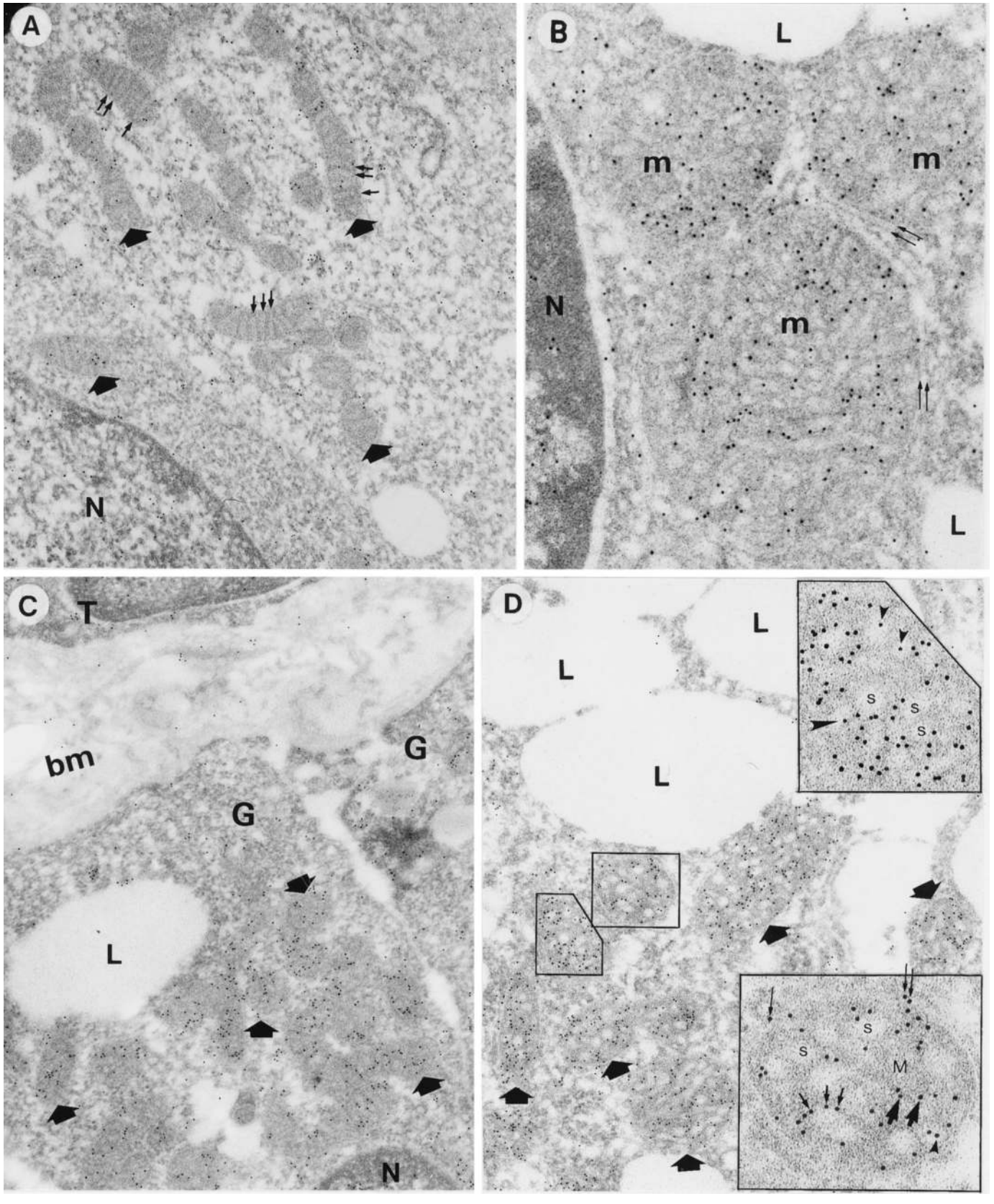

FIG. 6. Ultrastructural localization of ovarian StAR after PMSG/hCG treatment. At the indicated time points after hormone administration, ovaries were prepared for immuno-gold electron microscopy using antiserum to bacterially expressed StAR as described in *Materials and Methods*. In an attempt to preserve maximal antigenicity, sections were not osmicated and, therefore, the typical dark staining of the membrane

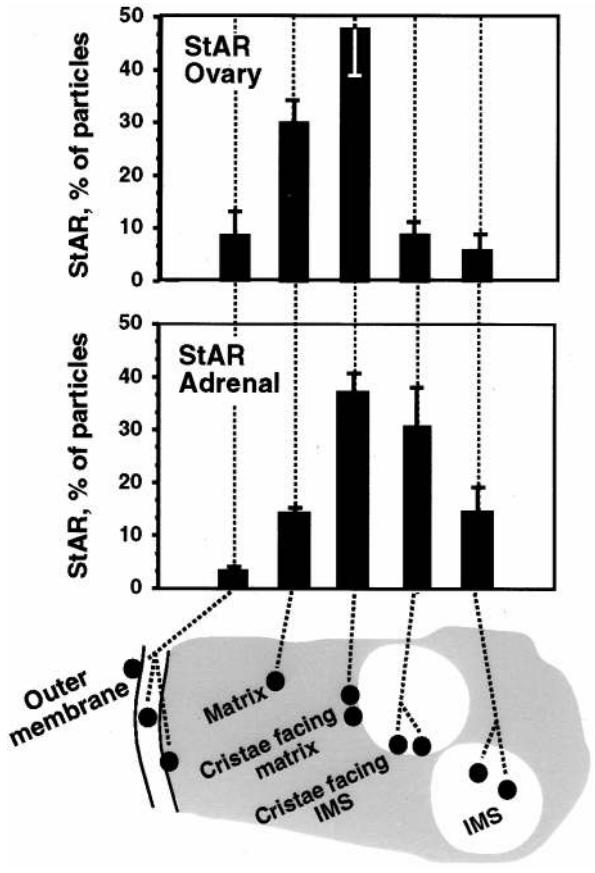

FIG. 7. Submitochondrial distribution of colloidal gold labeled StAR. *Upper panel*, 9 h after PMSG administration, colloidal gold particles were manually counted in 12 different high power photomicrographs of mitochondria from theca-interstitial cells (a typical example shown in *insets* of Fig. 6D). The electron micrographs were taken from five different cells in two different tissue blocks. The localization of the particles in the various submitochondrial compartments is illustrated and included the following categories: outer membrane-associated particles; matrix-located particles; cristae membrane bound particles facing the matrix; membrane-bound particles facing the intermembranes spaces; and particles located in the intermembranes spaces (IMS). *Lower panel*, Similar analysis performed for six mitochondria of rat adrenal fasciculata cells labeled with the same StAR antiserum used above (rabbit antiserum to bacterially expressed murine StAR). Data are presented as the percentage (mean + SD) of gold particles in the submitochondrial compartments of each mitochondion. A total of 1197 and 721 particles was counted for the analyses shown in the *upper* and the *lower* panels, respectively.

correspond to the concentration of the gonadotropins found in the circulation (42–44). The latter hormones elicit an orchestrated temporal expression pattern of steroidogenic enzymes (45), including P450scc, P45017α and P450arom, which determine the ovarian production of progestins, androgens and estrogens, respectively (46–48). Following this rationale, our previous attempts to reveal the nature of the ovarian functional cyclicity focused on characterization of P450scc expression patterns during the process of follicular development (21, 28, 38). In light of the earlier observation that the catalytic activity of P450scc is inconsequential without an active delivery of substrate cholesterol to its site in the mitochondrion (49), we needed to reevaluate our former studies by following the expression patterns of the StAR protein, a newly discovered protein, which is implicated in the regulation of cholesterol uptake by the mitochondria (see reviews, Refs. 5, 50, 51).

StAR expression: the early response

Using the immature rat model, the present study demonstrates remarkably rapid and dynamic changes in StAR levels during follicular development. The unique biphasic pattern of StAR response to PMSG/hCG was corroborated by three experimental approaches, including RT-PCR, Western blot analyses, and immunohistochemistry. The last of these methodologies clearly indicated that the immediate response of the ovarian tissue to the administered hormones was confined to the interstitial cells in between the follicles, as well as in fewer islands of theca interna cells. StAR transcripts were readily observable within 2 h following hormone administration, whereas no such response could be detected for either of the three cytochrome P450s we monitored using the same RNA extracts, *i.e.* P450scc, P45017α, or P450arom. The rapid rise in StAR expression provides, therefore, the first *in vivo* example of the acute nature of StAR response in the rat ovary. Moreover, the initial burst of StAR expression, exclusively confined to the interstitial cells and some of the theca cells, is in agreement with our previous studies, which showed that in unprimed prepubertal rats, these androgen producing cells are endowed with both P450scc and a large reservoir of cholesterol-ester lipids (29, 38). Consequently, the present studies suggest that StAR expression in the interstitial cells completes the exsisting protein repertoire (52) needed for steroidogenesis and, thereby, drives androgen production in this ovarian compartment. In this respect,

lipid bilayers is not observed. A, Granulosa cell examined 9 h after administration of PMSG. With the exception of a few background particles, the mitochondria (*thick arrows*) were devoid of StAR labeling. Note the typical lamellar cristae (*small arrows*) of the nonsteroidogenic mitochondria (29). N, nucleus. Magnification, ×27, 125. B, A neighboring interstitial cell from the same section shown in A. Note ample StAR-associated gold particle labeling in the mitochondria (m); note the typical tubular-vesicular architecture of the cristae (29) in such steroidogenic mitochondria. *Arrow doublets* depict the outer and the inner membranes of the mitochondrion, where StAR is thought to confer its bioactivity. N, Nucleus; L, lipid droplets. Magnification, ×50, 575. C, Two mural granulosa cells (G) depicted in a periovulatory follicle, 8 h after hCG administration. This micrograph depicts the basal side of the granulosa cells, resting on the follicular basal membrane (bm). Note ample StAR labeling in the mitochondria (*thick arrows*). N, nucleus; L, lipid droplets; T, a theca cell resting on the outer side of the basement membrane. Magnification, ×27, 125. D, An interstitial cell from the same section shown in C. In such terminally differentiated steroidogenic cells, ample lipid droplets (L) are localized adjacent to mitochondria (*thick arrows*), heavily decorated with multiple gold particles bound to immunoreactive StAR. Also, note the vesicular morphology of the cristae in such cells. Magnification, ×34,125. *Insets* show a higher power view of the *boxed area* in D, defining five categories by which the distribution of the gold particles can be described, as has been analyzed before (14, 29, 39): gold particles localized on the region of the outer mitochondrial membranes (*long arrows*); gold particles (*large arrows*) localized in the *gray area* of the matrix (M); membrane-bound gold particles facing the matrix (*small arrows*); membrane-bound particles (*large arrowheads*) facing the white intermembrane spaces (S); gold particles (*small arrowhead*) localized in the midst of the intermembrane spaces. Magnification, ×105, 625.

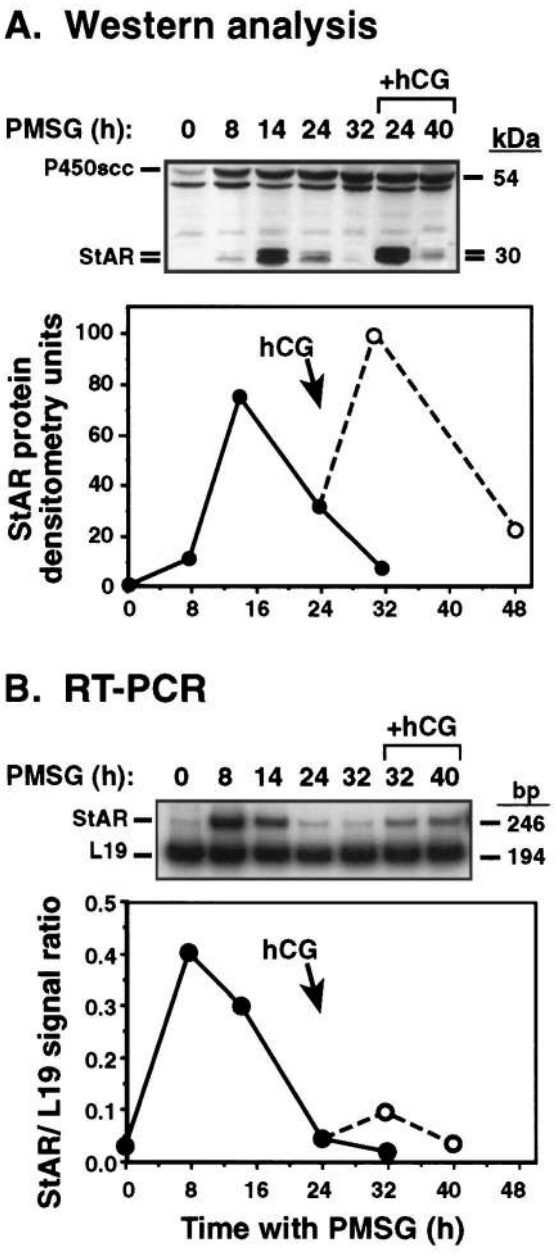

FIG. 8. Transient restoration of StAR expression obtained by premature hCG administration. PMSG (15 IU) was administered to immature rats, followed by a hCG (4 IU) boost given 24 h later. At the indicated time-points, protein and RNA extracts of whole ovarian tissue were prepared (*Materials and Methods*) and StAR products were determined by Western blot analysis (A) and RT-PCR (B) as described in the legends to Figs. 2 and 1, respectively. *Solid circles* and *lines* depict the gene product in control animals treated with PMSG only; *empty circles* and *broken lines* depict StAR products in animals receiving a premature hCG injection. The data represent one of two independent experiments repeated with similar results.

StAR expression in the ovarian interstitial cells probably resembles a similar scenario characterizing the constitutively active testicular androgen-producing Leydig cells, in which StAR level is upregulated in response to LH/hCG administration (32). Furthermore, in light of our results, it is tempting to speculate that in cells of the adrenal cortex, where proteins of the P450scc machinery are constitutively expressed at high levels (1, 53), diurnal changes in ACTH probably regulate StAR-mediated acute activation of steroidogenesis leading to the typical secretory patterns of cortisol in man (54).

Does the early rise in StAR expression generate *de novo* synthesis of androgens in the PMSG treated animal? Although we have not addressed this question by direct steroid measurements, positive and convincing evidence to this effect was reported more than two decades ago. Parker *et al.* (55) documented a 10-fold increase in serum androstenedione and testosterone, which were elevated within 12 h after PMSG administration to prepubertal animals; yet serum progesterone levels increased only 4-fold during the same time interval (55). However, based on later studies of steroid metabolism in this rat model, we now know that these reported androstenedione/testosterone levels must not have represented total androgen output because 5α-reduction of the aromatizable androgens to androsterone is a typical feature of the prepubertal rat ovary (25, 28). If so, what are the physiological consequences related to the early wave of StAR expression in the interstitial cells? The simple-minded assumption, that the interstitial cells provide androgens for estrogen production during this phase of follicular growth, is probably wrong, due to the fact that P450arom is not yet expressed during this early stage of follicular growth (Fig. 1 and Ref. 22). Instead, we would like to reinforce a previously proposed notion, that androgens can synergistically potentiate FSH-induced actions in the granulosa cells (56–59). Although the mechanism of such nonsubstrate action of androgens still remains ill-defined, thorough studies have demonstrated that aromatizable, as well as nonaromatizable, 5α-reduced androgens can markedly augment FSH induction of granulosa cell P450scc, P450arom, LH receptors, and PRL receptors (58, 59). Therefore, it is tempting to speculate that as a result of the early acute induction of StAR, the steroidogenically active interstitial tissue may support folliculogenesis by potentiating the effects of FSH on the functional maturation of the granulosa cell in leading follicles, be it either during onset of puberty, or during functional activation of a new cohort of follicles recruited for ovulation in cycling females. Richards and Bogovich (60, 61) have previously made a similar observation in support of this possibility, showing that a sustained administration of low doses of LH/hCG leads to a fully functional maturation of immature rat follicles. Therefore, it has been argued that, in the presence of the normal endogenous FSH secretion, the response to LH, and not FSH, appears to play the limiting event in the transition of follicles from the small antral stage to the preovulatory stage. Our results seem to be consistent with this notion. Furthermore, we wish to stress the contribution of the nonfollicular interstitial cells, which, in the face of the limited capacity of the theca-interna to express P450scc/StAR in the tertiary follicles, could possibly assume the role of androgen production until completion of the theca cell differentiation at later stages of follicular development.

Maturation of Graafian follicles is associated with StAR loss

The high levels of StAR elicited by PMSG administration did not remain for a long period of time in the mitochondria

of the interstitial cells. Following a substantial decline in StAR mRNA steady-state level, StAR protein levels decreased as well, with an apparent half-life of 10–12 h, which is significantly shorter than that previously determined for P450scc (36 h, Ref. 19, 62). Interestingly, attempts to restore StAR levels by a single boost of hCG administration transiently increased StAR protein to high levels in the mitochondria, but this increase was not associated with a marked effect on StAR mRNA (Fig. 8). In other words, the hCG boost seemed to trigger an increase in the translation of StAR from submaximal levels of StAR mRNA. In this respect, unlike the coupled biphasic waves of StAR mRNA and protein patterns described herein, the experimental manipulation of the ovary by the LH/hCG boost has provided *in vivo* circumstances to study the potential mode of transcription-independent induction of StAR protein synthesis. Such a possibility should be seriously considered as a feasible mode of StAR regulation in the ovary because many reports have claimed that the acute stimulation of adrenocorticosterone secretion by ACTH is resistant to inhibitors of transcription (63, 64).

It is not clear why StAR expression decreased following its initial burst in the interstitial cells. One possibility may be that steady-state StAR mRNA levels dropped as previously observed in stimulated MA-10 cells in culture (65). Therefore, it is possible that the decrease in StAR mRNA levels occurs as a natural consequence of StAR stimulation by hormones (65). Alternatively, a direct inhibitory effect on StAR expression should be considered as well. Such precedents have been previously reported for agents activating protein kinase C signaling pathway in cultured human granulosa cells (66), and luteolytic effects of $PGF_{2\alpha}$ in bovine corpora lutea (67). However, further studies are needed to determine if a negative mode of StAR regulation is a viable mechanism manipulating StAR expression during this stage of follicular development.

Surprisingly, the present study revealed that StAR was not expressed in the granulosa cells before hCG administration. A similar observation was recently made in heifers before ovarian hyperstimulation with eCG (68). This observation was not consistent with the high expression levels of P450scc documented in the granulosa cells of the Graafian follicles by Western blot analyses and immunohistochemical evidence (38). Therefore, if StAR truly determines the rate of steroidogenesis in the ovarian cells, these results imply that, at least in the immature rat undergoing PMSG-induced first ovulation, the *de novo* synthesis of androgen precursors needed for follicular estradiol production during the early to mid rat proestrus (42, 69), are not necessarily contributed by genuine cells of the follicle but rather by the secondary interstitial cells derived from atretic theca cells (70–73). We, therefore, wish to stress again the pivotal physiological role of these nonfollicular cells, which should receive more attention for their possible contributions as important, if not major, cellular sites for substrate supply for estrogen production by the Graafian granulosa cells.

Yet, the inverse correlation between the levels of P45017α and P450arom, both rising concomitantly, with the apparent decline in StAR levels before the timing of the LH surge, posed an apparent difficulty in explaining the need for StAR in facilitating the production of estrogen during the simulated proestrus period. Again, although we have not determined the levels of the ovarian steroids produced in our animal model, it should be stressed that the attenuation of StAR levels depicted in this study is consistent with a precipitous drop in serum progesterone monitored before the preovulatory LH-surge in both cycling rats (74) and the PMSG-treated rat model (55). Therefore, the inverse levels of proestrus progesterone and estrogen levels suggest that a relatively low rate of *de novo* steroidogenesis, possibly determined by StAR, is nevertheless sufficient to allow a maximal rate of estrogen synthesis, the serum levels of which are known to be two to three orders of magnitude lower than those of progesterone and androgens (42, 69, 74).

Orchestrated StAR expression in luteinizing follicles

The fidelity of StAR expression in the follicular cells was demonstrated once again following simulation of the LH surge by hCG administration; whereas high level of StAR expression was evident in the interstitium and theca interna cells of all follicles, in the granulosa cell compartment, the gonadotropin surge elicited an expression of StAR that was strictly confined to the periovulatory follicles. A similar pattern was previously observed under identical circumstances for granulosa cell expression of P450scc, which was exclusively confined to preovulatory and periovulatory follicles (38).

Interestingly, StAR levels peaked within 8 h after hCG administration, a period that has been previously defined as the critical time interval needed for the granulosa and the theca interna cells to pass the point of final commitment toward their terminal luteinization (22, 75, 76). The physiological role of StAR expression during this phase of follicular development can no longer relate to estrogen production, in lieu of the typical concomitant LH-induced loss of P45017α and P450arom expression (22, 77). Predominant progesterone production (42, 69, 74) becomes, therefore, the physiologically important ovarian event, which is tightly coupled to vigorous StAR expression and a transient expression of progesterone receptors (74, 78).

Finally, our survey concluded with the second decrease in ovarian StAR observed 12–14 h after hCG administration. This loss of StAR expression correlates well with the early estrus drop in circulating ovarian steroids (42, 69). As could be expected, StAR expression resumed in the active rat corpus luteum (Ronen-Fuhrman T. *et al.*, unpublished data), as has also been documented in mid-to-late cycle corpora lutea of numerous species, including human (66), bovine (79, 80), mouse (65), and rat (32, 81). We may, therefore, conclude that the dynamic changes in StAR expression in the rat ovary model are consistent with the ovarian steroidogenic output, if the cyclical rate of ovarian steroidogenesis is determined by StAR.

Intramitochondrial localization of StAR

The detailed mechanism by which StAR may facilitate cholesterol translocation to the mitochondrial inner membrane is still obscure. However, the observed ultrastructural localization of StAR in the ovarian mitochondria leads to intriguing, constructive conclusions. First, our immunoelectron microscopy studies revealed that a few hours after

PMSG administration, over 90% of StAR protein localized inside the mitochondrion rather than associated with potential contact sites of the outer membranes, where StAR is expected to function in its capacity to facilitate cholesterol entry. Moreover, the fate of StAR in the mitochondria was further demonstrated by the marked difference observed between the submitochondrial localization of hormone induced ovarian StAR and the gold labeling of StAR in the adrenal fasciculata tissue. Nine hours after PMSG induction, 77% of the ovarian StAR labeling was associated with the matrix milieu, whereas less than 15% of StAR antigens localized within the intermembrane spaces. By contrast, nearly 1:1 ratio of StAR labeling was observed in the adrenal, where over 45% of StAR antigens were spatially localized within the intermembrane spaces and similar levels of the gold particles labeled the mitochondrial matrix and the matrix face of the cristae membranes. The reasons for these tissue-specific differences in StAR distribution are not clear at present.

Altogether, these observations implied that StAR precursor remains on the mitochondrial surface for a relatively short time before it is processed upon its entry into the mitochondrion via its signal peptide. In light of this observation, it is tempting to assume that the intramitochondrial pool of StAR is biologically inactive and, therefore, cholesterol translocation is expected to depend on hormone induced synthesis of new StAR precursor molecules that are removed from the surface by means of its import and processing to yield the final 30-kDa mature mitochondrial form (5, 6). Therefore, such a model would be in agreement with the long-observed rapid inhibition of adrenal steroidogenesis following cycloheximide administration (49, 63, 82–84), yet suggests a slightly modified perception of StAR's mechanism of action. On a time scale of minutes, StAR is not necessarily a short-lived protein, but is better described as a protein of a short-lived function, the active form of which is rapidly transformed by the mitochondrial import process.

In summary, the present study suggests that, during hormone induced follicular development in the rat, expression of the ovarian StAR is upregulated during two relatively narrow time intervals. The first wave of StAR expression is predominantly occurring in the nonfollicular androgenic interstitial tissue, whereas the second burst of StAR expression responds to the LH surge, generating a concerted appearance of this protein in the granulosa and theca interna compartments of the dominant follicles. Although we have applied an artificial stimulation of follicular development in this animal model, the observed pattern of StAR expression can potentially explain some long-standing enigmatic fluctuations of the ovarian steroid hormone output previously documented during the normal reproductive cycle of the rats. Obviously, a direct corroboration of ovarian StAR patterns during the normal estrous cycle in adult rat, still awaits further studies. Yet, our study supports the notion that, similar to the adrenal and testis, StAR probably plays an obligatory role in supporting the ovarian steroidogenic capacity. Moreover, the spatio-temporal nature of StAR expression further emphasizes the concept that ovarian steroidogenic output is a result of a well orchestrated functional collaboration between the different ovarian cell types.

References

1. **Simpson ER, Waterman MR** 1988 Regulation of the synthesis of steroidogenic enzymes in adrenal cortical cells by ACTH. Annu Rev Physiol 50:427–440
2. **Richards JS, Hedin L** 1988 Molecular aspects of hormone action in ovarian follicular development, ovulation, and luteinization. Annu Rev Physiol 50:441–463
3. **Hall PF** 1986 Cytochromes P-450 and the regulation of steroid synthesis. Steroids 48:133–196
4. **Miller WL** 1988 Molecular biology of steroid hormone synthesis. Endocr Rev 9:295–318
5. **Stocco DM, Clark BJ** 1996 Regulation of the acute production of steroids in steroidogenic cells. Endocr Rev 17:221–244
6. **Stocco DM** 1997 A StAR search: implications in controlling steroidogenesis. Biol Reprod 56:328–336
7. **Stocco DM** 1997 The steroidogenic acute regulatory (StAR) protein two year later: an update. Endocrine 6:99–109
8. **Privalle CT, Crivello JF, Jefcoate CR** 1983 Regulation of intramitochondrial cholesterol transfer to side-chain cleavage cytochrome P450scc in rat adrenal gland. Proc Natl Acad Sci USA 80:702–706
9. **Pon LA, Orme-Johnson NR** 1988 Acute stimulation of corpus luteum cells by gonadotropin or adenosine 3′5′-monophosphate causes accumulation of a phosphoprotein concurrent with acceleration of steroid synthesis. Endocrinology 123:1942–1948
10. **Stocco DM, Sodeman TC** 1991 The 30-kDa mitochondrial proteins induced by hormone stimulation in MA-10 mouse Leydig tumor cells are processed from larger precursors. J Biol Chem 266:19731–19738
11. **Lin D, Sugawara T, Strauss JF, Clark BJ, Stocco DM, Sanger P, Rogol A, Miller WL** 1995 Role of steroidogenic acute regulatory protein in adrenal and gonadal steroidogenesis. Science 267:1828–1831
12. **Hauffa PT, Miller WL, Grumbach MM, Conte FA, Kaplan SL** 1985 Congenital adrenal hyperplasia due to deficient cholesterol side-chain cleavage activity (20, 22-desmolase) in a patient treated for 18 years. Clin Endocrinol 23:481–493
13. **Clark BJ, Wells J, King SR, Stocco DM** 1994 The purification, cloning and expression of a novel LH-induced mitochondrial protein in MA-10 mouse Leydig tumor cells: characterization of the steroidogenic acute regulatory protein (StAR). J Biol Chem 269:28314–28322
14. **King SR, Ronen-Fuhrmann T, Timberg R, Clark BJ, Orly J, Stocco DM** 1995 Steroid production following the *in vitro* transcription, translation and mitochondrial processing of the protein products of the cDNA for the steroidogenic acute regulatory (StAR) protein. Endocrinology 136:5165–5176
15. **Epstein LF, Orme-Johnson NR** 1991 Regulation of steroid hormone biosynthesis: identification of precursors of a phosphoprotein targeted to the mitochondrion in stimulated rat adrenal cortex cells. J Biol Chem 266:19739–19745
16. **Dohler KD, Wuttke W** 1975 Changes in levels of serum gonadotropins, prolactin and gonadal steroids in prepubertal male and female rats. Endocrinology 97:898–907
17. **Hsueh AJW, Adashi EY, Jones PBC, Welsh TH** 1984 Hormonal regulation of the differentiation of cultured ovarian granulosa cells. Endocr Rev 5:76–126
18. **Baird DT** 1977 Evidence *in vivo* for the two-cell hypothesis of oestrogen synthesis by the sheep Graafian follicle. J Reprod Fertil 50:183–185
19. **Goldring NB, Orly J** 1985 Concerted metabolism of steroid hormones produced by co cultured ovarian cell types. J Biol Chem 260:913–921
20. **Goldring NB, Farkash Y, Goldschmit D, Orly J** 1986 Immunofluorescence probing of the mitochondrial cholesterol side-chain cleavage cytochrome P-450 expressed in differentiating granulosa cells in culture. Endocrinology 119: 2821–2832
21. **Goldschmit D, Kraicer P, Orly J** 1989 Periovulatory expression of cholesterol side chain cleavage cytochrome P-450 in cumulus cells. Endocrinology 124:369–378
22. **Richards JS** 1994 Hormonal control of gene expression in the ovary. Endocr Rev 15:725–751
23. **Erickson GF, Wang C, Hsueh AJW** 1979 FSH induction of functional LH receptors in granulosa cells cultured in a chemically defined medium. Nature 279:336–339
24. **Segaloff, Wang H, Richards JS** 1990 Hormonal regulation of LH/chronic gonadotropin receptor mRNA in rat ovarian cells during follicular development and luteinization. Mol Endocrinol 4:1856–1865
25. **Erickson GF, Magoffin DA, Dyer CA, Hofeditz C** 1985 The ovarian androgen producing cells: A review of structure/function relationship. Endocr Rev 6:371
26. **Uilenbroek JT, Richards JS** 1979 Ovarian follicular development during the rat estrus cycle: gonadotropin receptors and follicular responsiveness. Biol Reprod 20:1159–1165
27. **Hsueh AJW, Billig H, Tsafriri A** 1994 Ovarian follicular atresia: a hormonally controlled apoptosis process. Endocr Rev 15:707–724
28. **Bitzur S, Orly J** 1989 Microanalysis of hormone responsive ovarian interstitial gland cells in miniature culture. Endocrinology 124:1471–1484
29. **Farkash Y, Timberg R, Orly J** 1986 Preparation of antiserum to rat cytochrome P-450 side chain cleavage and its use for ultrastructural localization of the immuno-reactive enzyme by protein A-gold technique. Endocrinology 118: 1353–1365
30. **Orly J, Rei Z, Greenberg N, Richards JS** 1994 Tyrosine kinase inhibitor AG18

arrests FSH induced granulosa cell differentiation: use of semi-quantitative RT-PCR assay for multiple mRNAs. Endocrinology 134:2336–2346
31. **Orly J, Clemens JW, Singer O, Richards JS** 1996 Effects of hormones and protein kinase inhibitors on expression of steroidogenic enzyme promoters in electroporated primary rat granulosa cells. Biol Reprod 54:208–218
32. **Sandhoff TW, McLean MP** 1996 Hormonal regulation of steroidogenic acute regulatory (StAR) protein messenger ribonucleic acid expression in the rat ovary. Endocrine 4:259–267
33. **Zor T, Selinger Z** 1996 Linearization of the Bradford protein assay increases its sensitivity: theoretical and experimental studies. Anal Biochem 236:302–308
34. **Laemmli UK** 1970 Cleavage of structural proteins during the assembly of the head of bacteriophage T4. Nature 227:680–685
35. **Otter T, King SM, Witman GB** 1987 A two-step procedure for efficient electrotransfer of both high-molecular weight (>400,000) and low-molecular weight (>20,000) proteins. Anal Biochem 162:370–377
36. **Orly J, Sato G, Erickson GF** 1980 Serum suppresses the expression of hormonally induced functions in cultured granulosa cells. Cell 20:817–827
37. **Gomberg-Malool S, Rei Z, Re'em Y, Posner I, Levitzki A, Orly J** 1993 Tyrphostins inhibit follicle stimulating hormone-mediated functions in cultured rat ovarian granulosa cells. Endocrinology 132:362–370
38. **Zlotkin T, Farkash Y, Orly J** 1986 Cell specific expression of immunoreactive cholesterol side chain cleavage cytochrome P-450 during follicular development in the ovary. Endocrinology 119:2809–2820
39. **Cherradi N, Rossier MF, Vallotton MB, Timberg R, Friedberg I, Orly J, Wang XJ, Stocco DM, Capponi AM** 1996 Submitochondrial distribution of three key steroidogenic proteins (steroidogenic acute regulatory protein, P450 side-chain cleavage and 3β-hydroxysteroid dehydrogenase isomerase enzymes) upon stimulation by intracellular calcium in adrenal glomerulosa cells. J Biol Chem 272:7899–7907
40. **Camp TA, Rahal JO, Mayo KE** 1991 Cellular localization and hormonal regulation of follicle stimulating hormone and luteinizing hormone receptor messenger RNAs in the rat ovary. Mol Endocrinol 5:1405–1417
41. **Chan Y-L, Lin A, McNally J, Peleg D, Meyuhus O, Wool IG** 1987 The primary structure of rat ribosomal protein L19. J Biol Chem 262:1111–1115
42. **Butcher RL, Collins WE, Fugo NW** 1974 Plasma concentration of LH, FSH, prolactin, progesterone and estradiol-17β throughout the 4-day estrus cycle of the rat. Endocrinology 94:1704–1708
43. **Richards JS** 1980 Maturation of ovarian follicles: actions and interactions of pituitary and ovarian hormones of follicular cell differentiation. Physiol Rev 60:51–89
44. **Abraham GE, Odell WD, Swerdloff RS** 1972 Simultaneous radioimmunoassay of plasma FSH, LH, progesterone, 17β-hydroxyprogesterone and estradiol-17β during the menstrual cycle. J Clin Endocrinol Metab 34:312–318
45. **Orly J** 1989 Orchestrated expression of steroidogenic side-chain cleavage cytochrome P450 during follicular development in the rat ovary. J Reprod Fert [Suppl] 37:155–162
46. **Hickey GJ, Chen S, Besman MJ, Shively JE, Hall PF, Gaddy-Kurten D, Richards JS** 1988 Hormonal regulation, tissue distribution, and content of aromatase cytochrome P450 messenger ribonucleic acid and enzyme in rat ovarian follicles and corpora lutea: relationship to estradiol biosynthesis. Endocrinology 122:1426–1436
47. **Miller WL** 1988 Molecular biology of steroid hormone synthesis. Endocr Rev 9:295–318
48. **Simpson ER, MacDonald PC** 1981 Endocrine physiology of the placenta. Annu Rev Physiol 43:163–188
49. **Simpson ER, McCarthy JL, Peterson JA** 1978 Evidence that the cycloheximide-sensitive site of adrenocorticotropic hormone action is in the mitochondrion: changes in pregnenolone formation, cholesterol content, and the electron paramagnetic resonance spectra of cytochrome P-450. J Biol Chem 253:3135–3139
50. **Stocco DM, Clark BJ** 1996 Role of the steroidogenic acute regulatory protein (StAR) in steroidogenesis. Biochem Pharmacol 51:197–205
51. **Stocco DM** 1997 A StAR search: implications in controlling steroidogenesis. Biol Reprod 56:328–336
52. **Hanukoglu I, Hanukoglu Z** 1986 Stoichiometry of mitochondrial cytochrome P450, adrenodoxin and adrenodoxin reductase in adrenal cortex and corpus luteum. Eur J Biochem 157:27–31
53. **Miller WL, Tyrrell JB** 1995 The adrenal cortex. In: Felig P, Baxter J, Frohman L (eds) Endocrinology and Metabolism. McGraw Hill, New York, pp 555–711
54. **Gallagher TF, Yoshida K, Roffwarg HD** 1973 ACTH and cortisol secretory patterns in man. J Clin Endocrinol Metab 36:1058
55. **Parker Jr CR, Costoff A, Muldoon TG, Mahesh VB** 1976 Actions of pregnant mare serum gonadotropin in the immature female rat: correlative changes in blood steroids, gonadotropins, and cytoplasmic estradiol receptors of the anterior pituitary and hypothalamus. Endocrinology 98:129–138
56. **Erickson GF, Wang C, Hsueh AJW** 1979 FSH induction of functional LH receptors in granulosa cells cultured in a chemically defined medium. Nature 279:336–339
57. **Daniel SAJ, Armstrong DT** 1980 Enhancement of follicle-stimulating hormone-induced aromatase activity by androgens in cultured rat granulosa cells. Endocrinology 107:1027–1033
58. **Hillier SG, De Zwart FA** 1981 Evidence that granulosa cell aromatase induction/activation by follicle stimulating hormone is an androgen receptor-regulated process *in vitro*. Endocrinology 109:1303–1305
59. **Fitzpatrick SL, Richards JS** 1991 Regulation of cytochrome P450 aromatase messenger ribonucleic acid and activity by steroids and gonadotropins in rat granulosa cells. Endocrinology 129:1452–1462
60. **Richards JS, Bogovich K** 1987 Effects of human chorionic gonadotropin and progesterone on follicular development in the immature rat. Endocrinology 111:1429–1438
61. **Bogovich K, Richards JS, Reichert Jr LE** 1981 Obligatory role of luteinizing hormone (LH) in the initiating of preovulatory follicular growth in the pregnant rat: specific effects of human chorionic gonadotropin and follicle stimulating hormone on LH receptors and steroidogenesis in theca, granulosa and luteal cells. Endocrinology 109:860–867
62. **Boggaram V, Zuber MX, Waterman MR** 1984 Turnover of newly synthesized cytochromes P450scc, P450 11b and adrenodoxin in bovine adrenocortical cells in monolayers culture: effect of adrenocorticotropin. Arch Biochem Biophys 23:518–524
63. **Garren LD, Ney RL, Davis WW** 1965 Studies on the role of protein synthesis in the regulation of corticosterone production by adrenocorticotropic hormone *in vivo*. Proc Natl Acad Sci USA 53:1443–1451
64. **Vernikos-Danellis J, Hall M** 1965 Inhibition of adrenocortical responsiveness to ACTH by actinomycin D *in vivo*. Nature 207:766
65. **Clark BJ, Soo S-C, Caron KM, Ikeda Y, Parker KL, Stocco DM** 1995 Hormonal and developmental regulation of the steroidogenic acute regulatory protein. Mol Endocrinol 9:1346–1355
66. **Kiriakidou M, McAllister JM, Sugawara T, Strauss III JF** 1996 Expression of steroidogenic acute regulatory protein (StAR) in the human ovary. J Clin Endocrinol Metab 81:4122–4128
67. **Juengel JL, Meberg BM, Turzillo AM, Nett TM, Niswender GD** 1995 Hormonal regulation of messenger ribonucleic acid encoding steroidogenic acute regulatory protein in ovine corpora lutea. Endocrinology 136:5423–5429
68. **Soumano K, Price CA** 1997 Ovarian follicular steroidogenic acute regulatory protein, low density lipoprotein receptor, and cytochrome P450 side chain cleavage messenger ribonucleic acids in cattle undergoing superovulation. Biol Reprod 56:516–522
69. **Smith MS, Freeman ME, Neill JD** 1975 The control of progesterone secretion during the estrous cycle and early pseudopregnancy in the Rat: Prolactin, Gonadotropin and steroid levels associated with rescue of the corpus luteum of pseudopregnancy. Endocrinology 96:219–227
70. **Tsafriri A, Braw RH** 1984 Experimental approaches to atresia in mammals. Oxford Rev Reprod Biol 6:226.45
71. **Dahl E** 1971 Studies of the fine structure of ovarian interstitial tissue. J Anat 108:275
72. **Taya K, Saidapur SK, Greenwald GS** 1980 Interstitium: Site of steroid synthesis in the ovary of the long term hypophysectomized hamster. Biol Reprod 22:307
73. **Carithers JR** 1976 Ultrastructure of rat ovarian interstitial cells: Response to luteinizing hormone. J Ultrastruct Res 55:96
74. **Park OK, Mayo KE** 1991 Transient expression of progesterone receptor messenger RNA in ovarian granulosa cells after the preovulatory luteinizing hormone surge. Mol Endocrinol 5:967–978
75. **Oonk RB, Krasnow JS, Beattie WG, Richards JS** 1989 1989 Cyclic AMP-dependent and independent regulation of cholesterol side-chain cleavage P450 (P450scc) in rat ovarian granulosa cells and corpora lutea. J Biol Chem 264:21934–21942
76. **Richards JS, Hedin L, Caston L** 1986 Differentiation of rat ovarian theca cells: evidence for functional luteinization. Endocrinology 118:1660–1668
77. **Weiss M, Eckstein B** 1984 Periovulatory changes in steroid C17,20-lyase activity in ovaries of immature rats treated with pregnant mare serum gonadotropin. Endocrinology 114:1912–1916
78. **Natraj U, Richards JS** 1993 Hormonal regulation, localization and functional activity of the progesterone receptor in granulosa cells of rat preovulatory follicles. Endocrinolgy 133:761–769
79. **Hartung S, Rust W, Balvers M, Ivell R** 1995 Molecular cloning and the *in vivo* expression of the bovine steroidogenic acute regulatory protein. Biochem Biophys Res Commun 215:649–653
80. **Pescador N, Soumano K, Stocco DM, Price CA, Murphy BD** 1996 Steroidogenic Acute Regulatory protein in bovine corpora lutea. Biol Reprod 55:485–491
81. **Sandhoff TW, McLean MP** 1996 Prostaglandin $F_{2\alpha}$ reduces steroidogenic acute regulatory (StAR) protein messenger ribonucleic acid expression in the rat ovary. Endocrine 5:183–190
82. **Ferguson JJ** 1963 Protein synthesis and adrenocorticotropin responsiveness. J Biol Chem 238:2754–2759
83. **Schulster D, Richardson MC, Palfreyman JW** 1974 The role of protein synthesis in adrenocorticotrophin action: effect of cycloheximide and puromycin on the steroidogenic response of isolated adrenocortical cells. Mol Cell Endocrinol 2:17–29
84. **Stevens VL, Xu T, Lambeth JD** 1993 Cholesterol trafficking in steroidogenic cells: reversible cycloheximide-dependent accumulation of cholesterol in a pre-steroidogenic pool. Eur J Biochem 216:557–563